Divergent Coordination Chemistry: Parallel Synthesis of [2 × 2] Iron(II) Grid-Complex Tauto-Conformers

Bernhard Schäfer, Jean-François Greisch, Isabelle Faus, Tilmann Bodenstein, Ivan Šalitroš, Olaf Fuhr, Karin Fink, Volker Schünemann, Manfred M. Kappes, and Mario Ruben*

Abstract: *The coordination of iron(II) ions by a homoditopic ligand **L** with two tridentate chelates leads to the tautomerism-driven emergence of complexity, with isomeric tetramers and trimers as the coordination products. The structures of the two dominant $[Fe^{II}_4L_4]^{8+}$ complexes were determined by X-ray diffraction, and the distinctness of the products was confirmed by ion-mobility mass spectrometry. Moreover, these two isomers display contrasting magnetic properties (Fe^{II} spin crossover vs. a blocked Fe^{II} high-spin state). These results demonstrate how the coordination of a metal ion to a ligand that can undergo tautomerization can increase, at a higher hierarchical level, complexity, here expressed by the formation of isomeric molecular assemblies with distinct physical properties. Such results are of importance for improving our understanding of the emergence of complexity in chemistry and biology.*

*I*ncreases in the complexity of self-organizing systems can be considered to result from three features of the self-organization process, namely multiplicity, interconnection, and integration.[1] The first parameter, multiplicity, has recently been shown to play a central role in the formation of convergent and divergent two-dimensional (2D) coordination networks on metal surfaces.[2–11] In the low-multiplicity, convergent case, ditopic ligands of high symmetry form monolayer coordination networks with co-sublimed metal atoms, such as cobalt, on low-index metal surfaces.[9] The growth of highly regular and periodic arrangements is due to the preference for a single binding motif, which is enhanced by self-correction mechanisms. The lateral symmetry restrictions of low-index metal surfaces then result in monolayers with extremely high 2D periodicity and regularity. In the high-multiplicity, divergent case, the formation of products with inversion symmetry is avoided. The use of non-linear prochiral ligands that can undergo isomerization on the surface by restricted rotation about single bonds leads to the formation of robust, disordered coordination networks with transition-metal centers in different coordination environments.[10] This coordinative multiplicity originates from the parallel expression of different coordination modes, leading to strictly non-periodic string- or bifurcation-like coordination motifs with increasing complexity; such processes are referred to as divergent coordination chemistry.[10, 11]

Following the proposition that such self-organization processes are equally responsible for the dynamic generation of molecular and supramolecular diversity and complexity in three-dimensional (3D) bulk structures,[12–15] we herein report on the complexation of a homoditopic ligand with two tridentate chelates with iron(II) and the accompanying tautomerism-driven emergence of complexity. Whereas a number of ligands with tridentate chelates and tautomeric subunits have previously been described,[16–20] we are not aware of any examples that describe the presence of different tauto-conformers and the parallel formation of isomeric reaction products. For our studies, we designed a homoditopic ligand **L**, which consists of two tridentate 2-(1*H*-imidazol-2-yl)-6-(pyrazol-1-yl)pyridine units interlinked via a central benzo[1,2-*d*:4,5-*d'*]diimidazole bridge (magenta, Figure 1a).

[*] Dr. B. Schäfer, Dr. J.-F. Greisch, Dr. T. Bodenstein, Dr. O. Fuhr,
Priv.-Doz. Dr. K. Fink, Prof. Dr. M. M. Kappes, Prof. Dr. M. Ruben
Institut für Nanotechnologie
Karlsruher Institut für Technologie (KIT)
Hermann-von-Helmholtz-Platz 1
76344 Eggenstein-Leopoldshafen (Germany)
E-mail: Mario.Ruben@kit.edu

Dr. O. Fuhr
Karlsruhe Nano-Micro Facility (KNMF)
Karlsruher Institut für Technologie (KIT)
Hermann-von-Helmholtz-Platz 1
76344 Eggenstein-Leopoldshafen (Germany)

Prof. Dr. M. M. Kappes
Institut für Physikalische Chemie
Karlsruher Institut für Technologie (KIT)
Fritz-Haber-Weg 2, 76131 Karlsruhe (Germany)

Prof. Dr. M. Ruben
Institut de Physique et Chimie des Matériaux de Strasbourg (IPCMS)
CNRS-Université de Strasbourg
23, rue du Loess, BP 43, 67034 Strasbourg cedex 2 (France)

Dr. I. Faus, Prof. Dr. V. Schünemann
Fachbereich Physik, Technische Universität Kaiserslautern (TUK)
Erwin-Schrödinger-Strasse 46, 67663 Kaiserslautern (Germany)

Dr. I. Šalitroš
Institute of Inorganic Chemistry, Technology and Materials
Faculty of Chemical and Food Technology
Slovak University of Technology
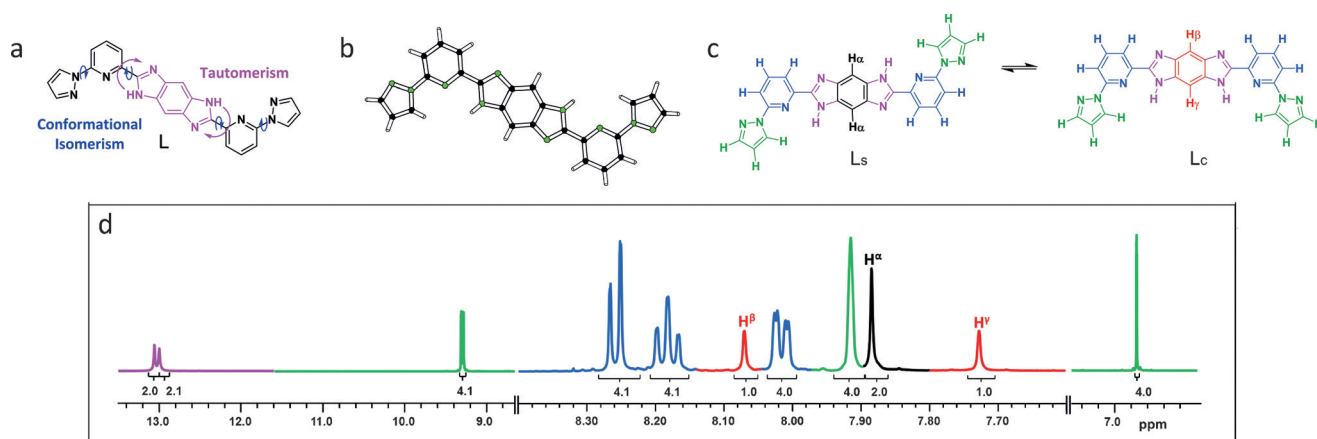Bratislava, 81237 (Slovak Republic)

Figure 1. a) The conformational isomerism and tautomerism of **L**. b) Molecular structure of **L$_s$** as determined by single-crystal X-ray diffraction (C black, H white, N green). c) The resulting **L$_S$** and **L$_C$** conformers of **L** as found in solution. d) ^{1}H NMR spectrum (in [D$_6$]-DMSO) showing the presence of **L$_S$** and **L$_C$** in a 1:1 ratio. The protons were assigned using the color codes shown in (c) and (d).

The bridging unit can (simultaneously) undergo two tautomerization processes of the secondary amine and imine functional groups. In addition, conformational isomers can be formed by rotation about the single bonds between the aromatic ring systems in the backbone of **L** (Figure 1 a). The rotation barriers of the single bonds connecting the pyridine and imidazole subunits enable two in-plane conformations, the so-called S and C conformations, **L$_S$** and **L$_C$** (this denomination arises from their apparent shape, see Figure 1 c).

Both tauto-conformers are able to coordinate metal ions in two tridentate binding pockets. The molecular structure of **L** was determined by single-crystal X-ray diffraction, which showed that **L** is present in its **L$_S$** form in the solid state (Figure 1 b). A solution sample of **L** was investigated by ^{1}H NMR spectroscopy, and the expected resonance sets for the peripheral pyrazole rings (green) and the neighboring pyridine rings (blue) could be identified. The central benzene moiety gives rise to three singlet resonances for the two H atoms with an integral ratio of 1:2:1 (Figure 1 d, red/black). Within the accuracy of ^{1}H NMR spectroscopy, the observed pattern can be attributed to the presence of the two tauto-conformers, **L$_S$**/**L$_C$**, in a 1:1 ratio in solution. Whereas the two benzene-based H atoms of the S conformer (H$^\alpha$) are equivalent with an

overall integral of 2H (Figure 1 d, black), the same two H atoms (H$^\beta$ and H$^\gamma$) are not equivalent in the C conformer, which leads to two separated singlet resonances with integration values of 1 H atom each (red). Additional evidence for an **L$_S$**/**L$_C$** ratio of 1:1 in solution is described in the Supporting Information.

The different chelating modes of **L** were read out by coordination of transition-metal ions. If the read-out takes place strictly in parallel,[10] multiple products differing in their structures and properties should be observed. The equimolar reaction of Fe^{II}(CF$_3$SO$_3$)$_2$ with **L** gives a red solution, as is typical for Fe^{II} polypyridyl systems. To get more insight, the
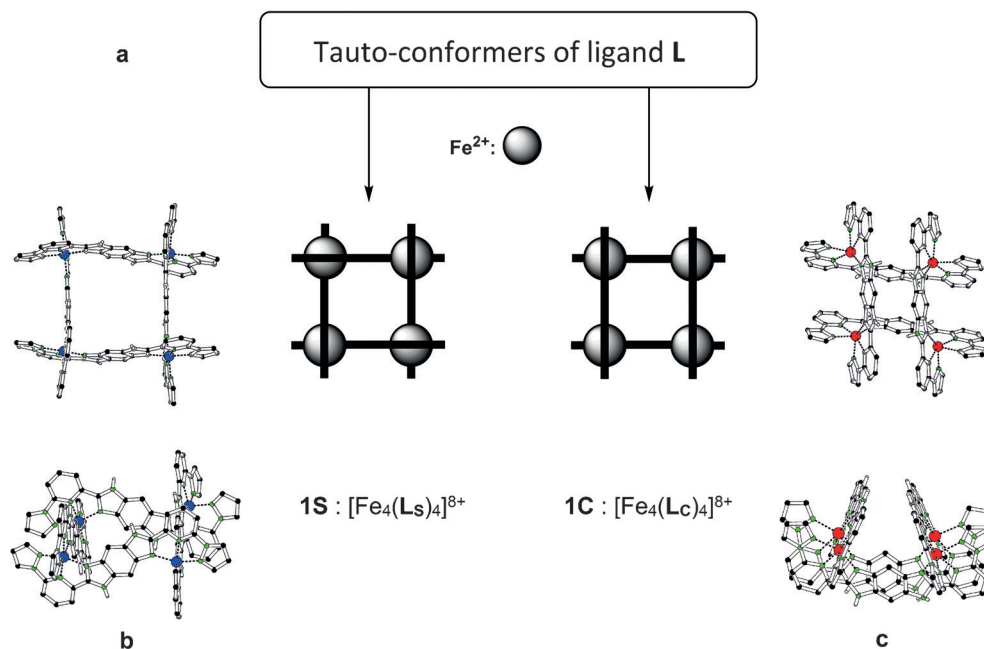

Figure 2. The coordination of **L** to Fe^{II} metal ions leads to the tautomerism-driven emergence of complexity. a) Schematic representation of the cationic moieties of the isolated isomers of the [2×2] Fe^{II}$_4$ grid complexes, consisting of **L** (black bars) and Fe^{II} ions (gray spheres). The molecular structures of the two [Fe$_4$L$_4$]$^{8+}$ tauto-conformers were determined by single-crystal X-ray diffraction. b) Top and side view of **1S**, c) top and side view of **1C** (C black, Fe HS red, Fe LS blue, N green).

crude solution was investigated by ESI-MS (see the Supporting Information, SI3.1, SIFig. 13, and SITable 1), which revealed the presence of tetrameric complexes of the type $[Fe_4L_4(CF_3SO_3)_x-yH]^{z+}$ ($z = 8-y-x$) as well as of trimers of the formula $[Fe_3L_3(CF_3SO_3)_x-yH]^{z+}$ ($z = 6-y-x$; see also Figure 3a). ^{1}H NMR studies confirmed the complex formation by revealing pronounced low-field shifts of the ligand resonances upon coordination of Fe[II] (SI3.2, SIFig. 14). The respective NH signals experienced a shift to 14 and 16 ppm, forming two different NH resonances in a ratio of 1:8. Two different, highly symmetric parameter sets are present in solution, representing two main molecular species. Fractional crystallization led to the complete removal of the minor species (SIFig. 15). The pure major fraction was studied by single-crystal X-ray diffraction, revealing the molecular structure of an interwoven [2×2] grid complex, **1S** (Figure 2b). The four Fe[II] ions are situated in distorted FeN_6 octahedra at the corners of a square while the ligands are arranged in an up–down pattern. At 180 K, all four Fe[II] ions form Fe–N bonds with lengths typical for low-spin (LS, $S = 0$) Fe[II] states. This finding was confirmed by the N-Fe-N bond angles, the sigma values (SI4.1, SITable 3),[21] and by magnetic studies (see below).

Upon short microwave heating of a solution of purified **1S**, a second paramagnetic signal set became visible in the ^{1}H NMR spectrum with an NH resonance at 15.9 ppm (SIFig. 16). Moreover, fractional crystallization of the microwave-irradiated mixture rendered crystals of the second major species. X-ray diffraction revealed the conformational isomer **1C**, in which the coordinated ligand **L** adapts the C conformation (Figure 2c). The average Fe–N bond lengths, N-Fe-N bond angles, and sigma values for **1C** indicate that at 180 K, all four Fe[II] ions are now in the HS state, in contrast to the situation found in **1S** at the same temperature. A detailed structural comparison of **1S** and **1C** is provided in SI4.1 and SIFig. 10.

To confirm the distinct character of **1S** and **1C** (to discriminate between two quickly interconverting species), we used ion-mobility mass spectrometry (IM-MS, see SI7), a technique that can spatially separate complex cations under the influence of an electric field by affecting their motion by collisions with a buffer gas.[22,23] In this particular case, travelling-wave IM-MS was used to identify the two conformational isomers **1S** and **1C**, which have identical masses (Figure 3a), by comparison of the experimentally inferred cross-sections and computed cross-sections based on DFT-optimized structures.[24,25] Assuming equal ionization efficiencies, the relative amounts of the two species can also be determined by deconvoluting the arrival time distributions (for details, see SI7) for the doubly charged **1C/1S** species $[Fe_4L_4-6H]^{2+}$ (Figure 3b) and integrating the corresponding peaks. Interestingly, a third, intermediate species (**IS**) could be detected as an additional peak at approximately 5.3 ms (SIFig. 25). The three species **1C/1S/IS** were present in relative amounts of about 65, 25, and 10%, respectively. The structure of **IS** appears to correspond to a tetramer with mixed L_S/L_C ligands (SIFig. 26,27).

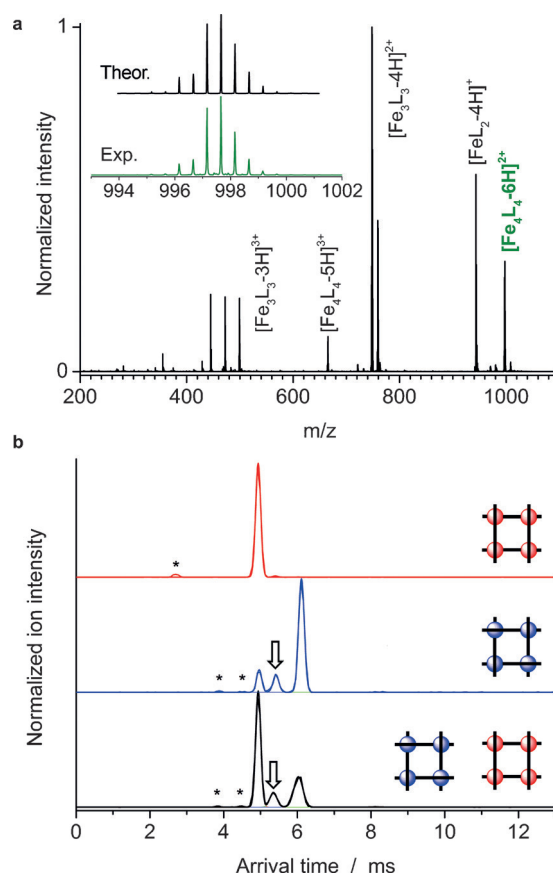To determine the magnetic properties of the tauto-conformers **1S** and **1C**, they were analyzed by temperature-

Figure 3. IM-MS analysis to distinguish the isomeric complexes (with identical *m/z* ratios). a) Mass spectrum (reaction solution) of **1**; peaks that are due to $[Fe_4L_4-6H]^{2+}$ are shown in green. b) Arrival time distributions (ATDs) for $[Fe_4L_4-6H]^{2+}$: **1C** (top, in red), **1S** (middle, in blue), and the as-synthesized mixture (bottom, in black); the arrows indicate an intermediate species (**IS**, for details see SI7).

dependent magnetometry (Figure 4a). The χT product of **1C** at room temperature gave a value of 13.2 cm³K mol⁻¹, and remained stable between 370–35 K. However, below 35 K, the χT value decreased rapidly, reaching a minimum value of 10 cm³K mol⁻¹ at 5 K. This drop was attributed to the zero-field splitting of the energy levels of the Fe[II] HS ions in an octahedral coordination environment. For mononuclear model complexes representing the two different Fe[II] centers of the [2×2] grid complex **1C**, the D tensors of the lowest quintet states as well as the Zeeman splittings of the five components were calculated by complete self-consistent field (CASSCF)[26] calculations and spin orbit configuration interaction (SOCI);[27] the magnetic field was included as a finite perturbation (for details, see SI8). By means of effective Hamiltonian theory,[28] we obtained D values of -30 cm⁻¹ and $D = -36$ cm⁻¹, respectively. These values were used as starting points for fitting the measured magnetic susceptibilities of **1C**, whereby the magnetic exchange couplings J_{ij} are assumed to be close to zero. A reasonable agreement with the experimental data was found by assuming that all centers have the same values for g (2.11) and D (-6 cm⁻¹) and an E/D value of 1/3 (see SIFig. 31, SITab. 4).
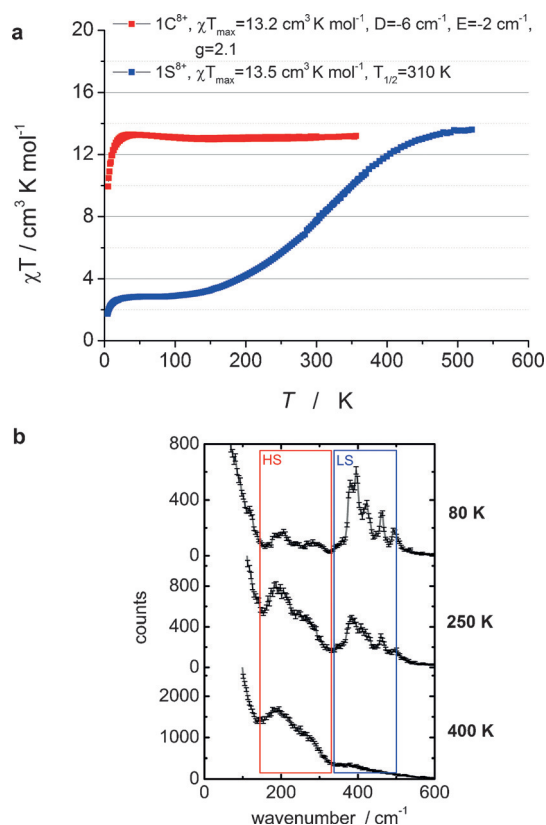
Figure 4. a) χT vs. temperature plots ($B = 0.1$ T) of **1C** (red) and **1S** (blue). b) Experimental nuclear resonance vibrational spectroscopy (NRVS) data of **1S** confirming the spin crossover behavior; the regions with spin marker bands for the HS and LS states are indicated by boxes.

For **1S**, a χT value of 13.5 cm³ K mol⁻¹ was measured at 520 K, but a gradual decrease with $T_{1/2} = 310$ K was observed upon decreasing the temperature; these are typical features of a spin crossover (SCO) process (for details, see SI4).[29] We can thus deduce from the magnetic susceptibility data that **1S** exhibits all typical features of SCO.[20] To confirm this result, a ⁵⁷Fe-enriched sample of **1S** was analyzed by nuclear resonance vibrational spectroscopy (NRVS; Figure 4b). The collected data led to the conclusion that **1S** has a diamagnetic ground state with all four Fe^{II} ions in the LS state at 80 K. At 250 K, SCO begins to take place, and is almost completed at 400 K, where all Fe^{II} ions are in the HS state. These results were also confirmed by the nuclear forward scattering data (see SI6/SIFig. 21).

The observed differences in the magnetic behavior of **1S** and **1C** can be understood as a direct consequence of the divergent coordination behavior of ligand **L**, which leads to the parallel emergence of two isomers with distinctly different physical properties, in our case exemplarily shown for the magnetic properties. The interwoven arrangement in complex **1S** reduces the distortion of the octahedral Fe{N₆} coordination polyhedra, thus favoring SCO behavior, whereas in **1C**, the backbones of two opposite C ligands point towards each other because of the intrinsic up–up/down–down coordination mode (see Figure 2). This strained arrangement leads to an additional distortion of the {N₆} ligand environment of the

Fe^{II} ions in **1C**, a situation that forces the Fe^{II} metal ions to remain in their HS state.

In conclusion, we have shown that after addition of Fe^{II} ions, the homoditopic ligand **L** renders increased multiplicity[1] by a tauto-isomerization process, expressing complexity through the formation of multiple coordination products. Among them, the two dominant isomeric tauto-conformers **1S** and **1C** of the [2×2] Fe^{II}_4 grid type could be isolated as crystals. The distinctness of the isomeric products **1S** and **1C** was confirmed by IM-MS in the gas phase, and their contrasting magnetic behavior was also analyzed, revealing the presence of Fe^{II} SCO for **1S** while **1C** is blocked in the HS state. The metastable product **1S** could be converted into the thermodynamic product **1C** by microwave heating. These results highlight how relatively simple molecular systems (here one homoditopic ligand **L**) can be turned into complex systems by the deconvolution of their inherent multiplicity following the rules of divergent coordination chemistry. In the future, additional parameters generating multiplicity, for example, chirality and stereoselectivity, will be included to improve our understanding of the emergence of complexity and hierarchy in chemistry and biology.

Acknowledgements

[1] J.-M. Lehn, *Angew. Chem. Int. Ed.* **2013**, *52*, 2836–2850; *Angew. Chem.* **2013**, *125*, 2906–2921.
[2] J.-M. Lehn, *Supramolecular Chemistry: Concepts and Perspectives*, VCH, Weinheim, New York, **1995**.
[3] J.-M. Lehn, *Proc. Natl. Acad. Sci. USA* **2002**, *99*, 4763–4768.
[4] J.-M. Lehn, *Science* **2002**, *295*, 2400–2403.
[5] M. Eigen, *Naturwissenschaften* **1971**, *58*, 465–523.
[6] M. Eigen, *Ber. Bunsen-Ges.* **1976**, *80*, 1059–1081.
[7] S. Lifson, *Biophys. Chem.* **1987**, *26*, 303–311.
[8] D. Newth, J. Finnigan, *Aust. J. Chem.* **2006**, *59*, 841.
[9] U. Schlickum, R. Decker, F. Klappenberger, G. Zoppellaro, S. Klyatskaya, M. Ruben, I. Silanes, A. Arnau, K. Kern, H. Brune et al., *Nano Lett.* **2007**, *7*, 3813–3817.
[10] M. Marschall, A. Weber-Bargioni, K. Seufert, W. Auwärter, S. Klyatskaya, G. Zoppellaro, M. Ruben, J. V. Barth, *Nat. Chem.* **2010**, *2*, 131–137.
[11] J. Čechal, C. S. Kley, T. Kumagai, F. Schramm, M. Ruben, S. Stepanow, K. Kern, *Chem. Commun.* **2014**, *50*, 9973–9976.

[12] J. T. Goodwin, D. G. Lynn, *J. Am. Chem. Soc.* **1992**, *114*, 9197–9198.

[13] J. R. Nitschke, J.-M. Lehn, *Proc. Natl. Acad. Sci. USA* **2003**, *100*, 11970–11974.

[14] R. Caraballo, H. Dong, J. P. Ribeiro, J. Jiménez-Barbero, O. Ramström, *Angew. Chem. Int. Ed.* **2010**, *49*, 589–593; *Angew. Chem.* **2010**, *122*, 599–603.

[15] M. Y. M. Abdelrahim, M. Tanc, J.-Y. Winum, C. T. Supuran, M. Barboiu, *Chem. Commun.* **2014**, *50*, 8043.

[16] T. Bark, M. Düggeli, H. Stoeckli-Evans, A. von Zelewsky, *Angew. Chem. Int. Ed.* **2001**, *40*, 2848–2851; *Angew. Chem.* **2001**, *113*, 2924–2927.

[17] J. I. van der Vlugt, S. Demeshko, S. Dechert, F. Meyer, *Inorg. Chem.* **2008**, *47*, 1576–1585.

[18] K. Kobayashi, M. Ishikubo, K. Kanaizuka, K. Kosuge, S. Masaoka, K. Sakai, K. Nozaki, M. Haga, *Chem. Eur. J.* **2011**, *17*, 6954–6963.

[19] J. E. Beves, J. J. Danon, D. A. Leigh, J.-F. Lemonnier, I. J. Vitorica-Yrezabal, *Angew. Chem. Int. Ed.* **2015**, *54*, 7555–7559; *Angew. Chem.* **2015**, *127*, 7665–7669.

[20] E. Breuning, M. Ruben, J.-M. Lehn, F. Renz, Y. Garcia, V. Ksenofontov, P. Gütlich, E. Wegelius, K. Rissanen, *Angew. Chem. Int. Ed.* **2000**, *39*, 2504–2507; *Angew. Chem.* **2000**, *112*, 2563–2566.

[21] B. Schäfer, C. Rajnák, I. Šalitros, O. Fuhr, D. Klar, C. Schmitz-Antoniak, E. Weschke, H. Wende, M. Ruben, *Chem. Commun.* **2013**, *49*, 10986.

[22] M. F. Mesleh, J. M. Hunter, A. A. Shvartsburg, G. C. Schatz, M. F. Jarrold, *J. Phys. Chem.* **1996**, *100*, 16082–16086.

[23] I. Campuzano, M. F. Bush, C. V. Robinson, C. Beaumont, K. Richardson, H. Kim, H. I. Kim, *Anal. Chem.* **2012**, *84*, 1026–1033.

[24] TURBOMOLE V6.6 2014, a development of the University of Karlsruhe and Forschungszentrum Karlsruhe GmbH, 1989–2007, TURBOMOLE GmbH, since 2007; available from http://www.turbomole.com.

[25] F. Weigend, *Phys. Chem. Chem. Phys.* **2006**, *8*, 1057.

[26] U. Meier, V. Staemmler, *Theor. Chim. Acta* **1989**, *76*, 95–111.

[27] K. Fink, C. Wang, V. Staemmler, *Inorg. Chem.* **1999**, *38*, 3847–3856.

[28] R. Maurice, R. Bastardis, C. de Graaf, N. Suaud, T. Mallah, N. Guihéry, *J. Chem. Theory Comput.* **2009**, *5*, 2977–2984.

[29] I. Šalitros, N. T. Madhu, R. Boča, J. Pavlik, M. Ruben, *Monatsh. Chem.* **2009**, *140*, 695–733.